Research Square

Preprints are preliminary reports that have not undergone peer review.
They should not be considered conclusive, used to inform clinical practice,
or referenced by the media as validated information.

Silencing OTUB1 promotes pyroptosis and M1 macrophages polarization to inhibit HepG2 cell proliferation

Yan Li

3292322114@qq.com

Second Affiliated Hospital of Harbin Medical University

Chen Hu

Second Affiliated Hospital of Harbin Medical University

Rui-Ling Xu

Second Affiliated Hospital of Harbin Medical University

Xin-Yu Geng

Second Affiliated Hospital of Harbin Medical University

Zhen-Dong Chen

Second Affiliated Hospital of Harbin Medical University

Jing Wang

Second Affiliated Hospital of Harbin Medical University

Ming-Na Liu

Second Affiliated Hospital of Harbin Medical University

Xin-Hong Wang

Second Affiliated Hospital of Harbin Medical University

Research Article

Keywords: OTUB1, pyroptosis, liver cancer, macrophage polarization, tumor microenvironment

Posted Date: July 3rd, 2026

DOI: https://doi.org/10.21203/rs.3.rs-9945441/v1

License: This work is licensed under a Creative Commons Attribution 4.0 International License.
Read Full License

Additional Declarations: No competing interests reported.

Abstract

Background

Liver cancer is a highly malignant tumor worldwide. Macrophage polarization in the tumor microenvironment critically influences cancer progression and immunity. Deubiquitinating enzyme OTUB1 regulates various tumor processes, but its role in pyroptosis remains unclear. This study investigates the effects of OTUB1 silencing on pyroptosis in HepG2 cells, macrophages, and co-culture systems.

Methods

The transfection efficiency of siRNA was evaluated using immunofluorescence and western blot. Cell proliferation was measured using the Cell Counting Kit − 8 (CCK-8), pyroptosis morphology was observed via electron microscopy, and the expression of pyroptosis-related proteins, inflammatory cytokines, and macrophage markers was detected by western blot. Co-immunoprecipitation (Co-IP) and mass spectrometry were used to identify potential OTUB1-interacting proteins. Statistical analysis and graphing were performed using GraphPad Prism.

Results

OTUB1 was effectively silenced at 72 h post-transfection. CCK-8 showed that the viability of HepG2 cells gradually increased in the co-culture group. In contrast, it decreased over time in the transfection and co-culture transfection groups, with the most pronounced effect observed at 72 h. The inhibition was further enhanced under co-culture. M0 macrophage viability decreased in the transfection group. Transmission electron microscopy revealed pyroptotic morphology in both HepG2 and M0 transfection groups. At 72 h, Cleaved-Caspase-4 and − 1 levels were elevated in HepG2 cells and M0 macrophages from the transfection and co-culture transfection groups, whereas GSDMD, IL-18, and IL-1β were decreased, with more pronounced changes in the co-culture transfection group. In co-cultured liver cancer cells, Cleaved-Caspase-4/1 decreased, while GSDMD, IL-18, and IL-1β increased. M0 macrophages differentiate into M2 macrophages in the co-culture group, while M0 macrophages differentiate into M1 macrophages in the co-culture transfection group. Co-IP and mass spectrometry identified a protein interaction network (including PSMC6, DDX17, LUC7L2, TUFM, RPS14/RPS24, ALDH2, ERP70, ACAA2, PRDX3) suggesting that OTUB1 may influence liver cancer cell functions through these interactions.

Conclusions

OTUB1 silencing promotes pyroptosis in both HepG2 cells and macrophages, induces M1 macrophage polarization, and thereby inhibits HepG2 cell proliferation. OTUB1 may be a key regulator of the

pyroptosis–macrophage polarization–liver cancer progression axis.

Introduction

Liver cancer is one of the malignant tumors with high incidence and high mortality worldwide [1,2]. The complex liver cancer microenvironment plays a critical role in the occurrence, progression, and therapeutic resistance of liver cancer [3,4]. Tumor-associated macrophages (TAMs) are among the most abundant immune cell populations in the liver cancer microenvironment, and their polarization status directly influences inflammatory responses, immune evasion, angiogenesis, as well as cell proliferation and migration [4–6]. Generally, M1-like macrophages exhibit pro-inflammatory and anti-tumor characteristics, whereas M2-like macrophages tend to be immunosuppressive and pro-tumorigenic [5–8].

Tumor growth is inseparable from cell proliferation and cell death. Pyroptosis, as a novel form of programmed cell death dependent on inflammasomes, has become a research hotspot due to its important role in regulating tumors, inflammation, and immunity [9–12]. Recent studies have shown that pyroptosis can not only directly affect tumor cell survival but also reshape the tumor microenvironment by releasing pro-inflammatory cytokines such as interleukin-1β (IL-1β) and IL-18, thereby influencing immune cell infiltration and function [10,13–15]. Therefore, the connection between pyroptosis and tumor immune regulation has become an important direction in liver cancer research. Moreover, some studies have found that macrophage pyroptosis may participate in the phenotypic transformation of TAMs by modulating the release of inflammatory cytokines [16,17].

Deubiquitinases participate in the regulation of cell death signaling pathways by dynamically modulating protein ubiquitination levels [18,19]. Ovarian tumor deubiquitinase, ubiquitin aldehyde binding 1 (OTUB1), as an important member of the OTU family of deubiquitinases, plays a significant role in maintaining protein homeostasis, DNA damage repair, inflammatory signaling, and tumor progression [20,21]. Current research indicates that OTUB1 promotes the progression of HCC by stabilizing receptor for activated C kinase 1 or antagonizing tripartite motif-containing 21-mediated sphingosine kinase 1 ubiquitination [22–24]. Notably, OTUB1 is aberrantly expressed in various tumors and is closely associated with cell proliferation, apoptosis, ferroptosis, and immune evasion [25–28]; however, its relationship with pyroptosis remains unclear. Our previous work found that silencing OTUB1 promotes pyroptosis in liver cancer cells. However, its effect on macrophages, particularly whether it can further regulate liver cancer cell behavior by influencing macrophage pyroptosis and polarization, has not been systematically investigated.

Based on the above, this study focuses on the central theme of "OTUB1 regulates pyroptosis, affects macrophage polarization, and thereby alters liver cancer cell growth." A co-culture system of HepG2 cells and THP-1-derived M0 macrophages will be established to systematically observe the effects of OTUB1 silencing on cell proliferation, pyroptosis-related molecules, and macrophage polarization phenotypes in both cell types.

Materials and methods

1. Materials

Both HepG2 and THP-1 cells were purchased from Abcell (Beijing, China). The small interfering RNA (siRNA) sequence targeting OTUB1 was designed as follows: sense (5'-3'): GCGACUCCGAAGGUGUUAATT; antisense (5'-3'): UUAACACCUUCGGAGUCGCTT, synthesized by General Biosystems Co., Ltd (Anhui, China). Lipofectamine™ 8000 was bought from Beyotime Biotechnology (Shanghai, China). The primary antibodies against OTUB1, Gasdermin D (GSDMD), Cleaved-Caspase-1, Cleaved-Caspase-4, Cluster of Differentiation 206 (CD206), and CD86, along with the Horseradish Peroxidase (HRP)-labeled goat anti-rabbit IgG (H + L) secondary antibody, were obtained from Immunoway (Beijing, China). The primary antibodies against IL-18, IL-1β, and β-actin were purchased from Abways (Shanghai, China). The Cell Counting Kit-8 (CCK-8) solution, Bicinchoninic Acid (BCA) kit, Enhanced Chemiluminescence (ECL) luminescent solution, and the magnetic beads for Co-immunoprecipitation (Co-IP) were purchased from Seven (Beijing, China). The primary antibody for OTUB1 used in Co-IP was purchased from Abmart (Shanghai, China), and the primary antibody for IgG was purchased from Proteintech (Chicago, USA).

2. Cell culture

HepG2 cells were cultured in flasks containing Dulbecco's Modified Eagle Medium (DMEM) medium with 10% fetal bovine serum, while THP-1 cells were cultured in flasks containing Roswell Park Memorial Institute (RPMI)-1640 medium with 10% fetal bovine serum. Both cultures were maintained in a constant temperature incubator at 37°C with 5% CO_2. THP-1 cells were treated with 100 ng/ml Phorbol 12-myristate 13-acetate (PMA) to achieve adhesion and differentiate into M0 macrophages. Adherent M0 macrophages were then incubated with 100 ng/ml lipopolysaccharide (LPS) and 20 ng/ml interferon-gamma (IFN-γ) for 48 hours to induce M1 polarization. Alternatively, adherent M0 macrophages were incubated with 20 ng/ml IL-4 and 20 ng/ml IL-13 for 48 hours to induce M2 polarization. When co-culturing HepG2 cells with M0 macrophages, the two cell types were respectively placed in the upper and lower chambers of a Transwell well, and incubated for 72 hours before use.

3. Cell Grouping

Based on different experimental requirements, the cells were divided into the HepG2 control group, HepG2 transfection group, M0 macrophage control group, M0 macrophage transfection group, co-culture group, co-culture transfection group, M1 macrophage group, and M2 macrophage group.

4. Cell transfection

When HepG2 and THP-1 cells were in good growth condition, we prepared the cell suspension and added 1 mL of the suspension per well to a 6-well plate. For THP-1 cells, we added 10 μL of PMA per well to induce them into M0 macrophages. After 24 hours of cell culture, the cell density reached 30% – 50%. Add a mixture containing 250 μL Opti-MEM, 5 μL OTUB1 siRNA, and 4 μL Lipo8000 to each well, and then mix thoroughly. The cells were cultured for approximately 10 hours before the culture medium was replaced with complete culture medium. Continue culturing for 72 hours, then collect the cells or extract proteins for subsequent experiments.

5. Verification of OTUB1 siRNA transfection efficiency by immunofluorescence

A suspension containing 1×10^5 HepG2 or THP-1 cells in good condition was prepared. 400 μl of the cell suspension was added to each well of a 24-well plate. THP-1 cells were induced to become M0 macrophages using PMA. After 24 hours of cell culture, the cell density was adjusted to 30%-50%. Each well was supplemented with a mixture containing 100 μl Opti-MEM, 2.5 μl fluorescent OTUB1 siRNA, and 1 μl Lipo 8000. The mixture was thoroughly mixed, and cell culture was continued. After 10 hours, the efficiency of siRNA transfection was assessed under a fluorescence microscope. Randomly select 5 high-power fields, count the number of cells, and calculate. Positive ratio (%) = (number of siRNA-positive cells / total number of cells) × 100%.

6. CCK-8 assay for detecting cell proliferation

(1) HepG2 cell experiment: HepG2 cells (3×10^3 cells/well) were seeded into 96-well plates and cultured until 30%–50% confluence. Six groups were established: control group (A), negative transfection group (B, transfected with negative siRNA), transfection group (C, transfected with OTUB1 siRNA), co-culture group (D), and co-culture transfection group (E, transfected with OTUB1 siRNA + co-culture conditioned medium). At 10 hours post-transfection, the medium was changed: groups A, B, and C received DMEM complete medium; group D received co-culture conditioned medium; group E received co-culture conditioned medium containing OTUB1 siRNA. CCK-8 solution was added at 24, 48, and 72 hours, and after incubation for 2–4 hours, OD450 was measured. The experiment was repeated three times, and growth curves were plotted.

(2) THP-1 cell experiment: THP-1 cells (3.5×10^3 cells/well) were seeded into 96-well plates and treated with PMA to induce differentiation into M0 macrophages until 30%–50% confluence. Three groups were established: control group (A), negative transfection group (B, transfected with negative siRNA), and transfection group (C, transfected with OTUB1 siRNA). Subsequent treatments (transfection and CCK – 8 detection) were the same as those for HepG2 cells.

7. Observation of pyroptosis morphology by electron microscopy

At 72 hours post-transfection, HepG2 cells and M0 macrophages from the control and transfection groups were collected. HepG2 cells were collected by trypsin digestion, and M0 macrophages were collected using a cell scraper. The collected cells were centrifuged at 1000 r/min for 5 minutes, the supernatant was discarded, and the pellet was resuspended and transferred to an EP tube, then centrifuged again at 3000 r/min for 15 minutes. The supernatant was discarded, and 1 mL of glutaraldehyde fixative was added to resuspend the pellet, which was then stored at 4°C for transmission electron microscopy.

8. Detection of protein expression by Western blot

At 72 hours post-transfection, total protein was extracted from each group, and protein concentration was determined using the Bicinchoninic Acid (BCA) Assay Kit method. Equal amounts of protein were separated by 10% sodium dodecyl sulfate (SDS)-polyacrylamide gel electrophoresis, and then transferred onto polyvinylidene fluoride (PVDF) membranes using a wet transfer system. After transfer, the membranes were blocked in protein-free rapid blocking solution for 15–20 minutes on a shaker at 37°C. After washing, the membranes were incubated with the corresponding primary antibodies at 4°C for 16–20 hours, then washed again and incubated with the corresponding secondary antibodies for 1 hour at room temperature. The blots were developed using an ECL chemiluminescence kit. Gray values were analyzed using ImageJ software, and graphs were generated using GraphPad Prism.

9. Detection of OTUB1 downstream genes by Co-IP and mass spectrometry

Well-grown HepG2 cells were seeded into 6-well plates. When cell confluence reached 70%–80%, cells were collected and washed twice with pre-chilled PBS. According to cell density, 100–120 μL of Radioimmunoprecipitation Assay (RIPA) lysis buffer containing protease inhibitors was added to each well, and cells were lysed on ice for 30 minutes. The lysates were then centrifuged at 12,000 r/min for 15 minutes at 4°C, and the supernatants were collected. After protein concentration determination by the BCA method, 60 μg of total protein from the experimental group was incubated with 2 μL of OTUB1-specific primary antibody, and 30 μg of total protein from the control group was incubated with 0.5 μL of IgG-specific primary antibody. Both were incubated overnight on a shaker at 4°C. The next day, Protein A/G magnetic beads were added to both groups and incubated for an additional 6 hours at 4°C, after which the beads were collected using a magnetic stand. After washing, the immunoprecipitated products were sent for mass spectrometry analysis. The mass spectrometry was completed by Novogene Bioinformatics Technology Co., Ltd (Beijing, China).

10. Statistical analysis

All experiments were repeated three times. Gray values of Western blot bands were quantitatively analyzed using ImageJ, and statistical analysis and graphing were performed using GraphPad Prism. For comparisons between two groups, Student's t-test was used. For comparisons among three or more groups (including four groups), one-way ANOVA was used. A P-value < 0.05 was considered statistically significant.

Results

1. Validation of siRNA transfection efficiency by immunofluorescence

Fluorescently labeled OTUB1 siRNA was transfected into HepG2 cells and M0 macrophages. At 10 hours post-transfection, fluorescence microscopy revealed clear green fluorescent signals in both 4× and 20× fields; under 20× magnification, the fluorescence appeared as intracellular punctate distribution. More than 90% of HepG2 cells and M0 macrophages exhibited green fluorescence (Fig. 1), indicating efficient uptake of the fluorescently labeled OTUB1 siRNA by the cells, providing a reliable basis for subsequent gene knockdown and functional experiments.

2. Validation of OTUB1 silencing efficiency by Western blot

OTUB1 siRNA and negative control siRNA were transfected into HepG2 cells and M0 macrophages for 72 hours. Western blot analysis showed that OTUB1 protein expression was effectively downregulated in the transfection groups for both cell types ($P < 0.05$) (Fig. 2), while no significant change was observed in the negative control groups, indicating that OTUB1 siRNA efficiently silenced OTUB1 protein expression in HepG2 cells and M0 macrophages.

3. Detection of cell proliferation by CCK-8 assay

CCK-8 results for HepG2 cells (Fig. 3) showed that cell viability in the control group and negative transfection group increased gradually over time, with no significant difference, suggesting that negative siRNA had minimal effects. In the OTUB1 silencing transfection group, the OD value at 72 hours was significantly lower than those in the control and negative transfection groups ($P < 0.05$), indicating that OTUB1 silencing inhibits HepG2 cell proliferation. After co-culture with M0 macrophages, HepG2 cell viability was higher than that in the control group at all time points ($P < 0.05$), suggesting that co-culture with macrophages promotes HepG2 cell proliferation. In contrast, when co-culture was performed under OTUB1 silencing conditions, HepG2 cell viability was overall lower than that in the transfection group (Group C), with the most obvious decrease at 72 hours, indicating that OTUB1 silencing enhances the inhibitory effect of macrophages on HepG2 proliferation.

CCK-8 results for M0 macrophages showed no significant difference in cell viability between the control and negative transfection groups ($P > 0.05$); however, cell viability in the OTUB1 silencing group was significantly reduced ($P < 0.05$) (Fig. 3), indicating that OTUB1 silencing inhibits M0 macrophage proliferation.

4. Observation of pyroptosis morphology by electron microscopy

At 72 hours after transfecting OTUB1 siRNA into HepG2 cells and M0 macrophages, cells were collected and observed by transmission electron microscopy. The transfection groups displayed typical pyroptotic morphology, including cell swelling, nuclear pyknosis or even rupture, plasma membrane rupture, and cytoplasmic vacuolation (Fig. 4).

5. Expression of pyroptosis markers and inflammatory cytokines in liver cancer cells and M0 macrophages after OTUB1 silencing

At 72 hours post-transfection, proteins were collected from each group, and Western blot was used to detect pyroptosis-related proteins and inflammatory cytokines. The results (Fig. 5) showed that in both HepG2 cells and M0 macrophages, OTUB1 silencing increased the expression of Cleaved-Caspase-1 and Cleaved-Caspase-4, while decreasing the expression of GSDMD, IL-18, and IL-1β ($P < 0.05$), indicating that OTUB1 silencing activates the pyroptosis pathway in both cell types. In the co-culture group, Cleaved-Caspase-1/4 decreased, while GSDMD, IL-18, and IL-1β increased ($P < 0.05$), suggesting that co-culture with macrophages inhibits HepG2 pyroptosis, favoring liver cancer growth. In contrast, after OTUB1 silencing under co-culture conditions, the above trend was reversed (Cleaved-Caspase-1/4 increased, GSDMD and inflammatory cytokines decreased, $P < 0.05$), indicating that after OTUB1 silencing, macrophages promote pyroptosis activation in HepG2 cells. In summary, OTUB1 silencing promotes pyroptosis in HepG2 cells; co-culture with macrophages inhibits HepG2 pyroptosis; and OTUB1 silencing reverses the inhibitory effect of co-culture, turning it into promotion of HepG2 pyroptosis.

6. Changes in M0 macrophage polarization markers after OTUB1 silencing

At 72 hours post-transfection, proteins were collected from each group, and Western blot was used to detect the macrophage markers CD86 (M1 type) and CD206 (M2 type). The results (Fig. 6) showed that compared with the control group, the transfection group exhibited decreased CD86 expression with no significant change in CD206; the co-culture group showed decreased CD86 and increased CD206 expression, with no significant difference from M2-type macrophages ($P > 0.05$), indicating that co-culture induces M0 macrophages to polarize toward the M2 phenotype. In the co-culture transfection group, CD86 and CD206 expression showed no significant difference from either M1 or M0 groups ($P > 0.05$). Combined with the changes in HepG2 cells, this suggests a possible shift toward M1 polarization, but further verification is needed.

7. Identification of OTUB1 downstream genes by Co-IP and mass spectrometry

Co-IP results showed that the IP group contained significantly more specific proteins (2922) than the IgG control group (1143), with 921 overlapping proteins (Fig. 7). GO annotation analysis indicated that the identified proteins were mainly enriched in biological processes such as redox, transport, and translation, as well as in cellular components including the nucleus, membrane, and cytoplasm, suggesting that OTUB1 may exert regulatory functions through multiple cellular activities (Fig. 7). KEGG pathway analysis revealed that the proteins were mainly enriched in cellular processes, genetic information processing, and human disease-related pathways, particularly pathways related to hepatocellular carcinoma development and progression, including cell growth, death, and cancer pathways (Fig. 7). Further construction of a protein-protein interaction (PPI) network revealed approximately 59 nodes, with PSMC6, DDX17, LUC7L2, TUFM, RPS14/RPS24, ALDH2, ERP70, ACAA2, PRDX3, and others occupying central positions (Fig. 7).

Discussion

This study systematically investigated the biological changes in liver cancer cells and macrophages following OTUB1 silencing, centered on the theme of “OTUB1-pyroptosis-macrophage polarization-liver cancer cell growth”. In our experiments, CCK-8 results showed that OTUB1 silencing inhibited the proliferation of HepG2 cells and M0 macrophages. Transmission electron microscopy revealed that OTUB1 silencing promoted pyroptosis in both HepG2 cells and M0 macrophages. These findings indicated that silencing OTUB1 promotes pyroptosis and thereby suppresses cell proliferation.

Pyroptosis, an inflammatory form of programmed cell death, involves a core process: cleavage and activation of caspase-1 (canonical pathway) or caspase-4/5 (non-canonical pathway) → cleavage of GSDMD to form membrane pores → cell swelling and membrane rupture → maturation/release of inflammatory cytokines such as IL-1β and IL-18 [29]. This process may directly inhibit tumor cell survival and reshape the immune microenvironment through inflammatory signals [30]. In this study, after OTUB1 silencing, elevated levels of Cleaved-caspase-1 and Cleaved-caspase-4 indicate increased pyroptosis. However, the levels of GSDMD, IL-1β, and IL-18 unexpectedly decreased. Combined with the pyroptotic morphology observed by transmission electron microscopy, we hypothesize that this result may be related to the endpoint detection time window. At later stages of pyroptosis, relevant proteins may be cleaved, consumed, or released into the extracellular space, leading to decreased intracellular detection levels. Therefore, our findings support an overall interpretation that the “pyroptosis-related pathway is activated”, rather than a linear explanation based solely on the direction of change of any single protein. Further dynamic validation using supernatant IL-1β/IL-18 release, and GSDMD cleavage fragments is needed.

It is well known that tumors promote the M2 polarization of macrophages, which in turn promotes tumor growth [31,32]. In contrast, M1-polarized macrophages inhibit tumor growth [8]. Our results are

consistent with these observations. In this experiment, M0 macrophages in the co-culture group underwent M2 polarization, promoting HepG2 cell proliferation; whereas M0 macrophages in the OTUB1-silenced co-culture group exhibited M1 polarization, inhibiting HepG2 cell proliferation. This suggests that OTUB1 may not act solely on tumor cells themselves, but also participates in shaping the immune phenotype within the tumor microenvironment. OTUB1 may influence liver cancer cell behavior by regulating macrophage polarization, providing a novel perspective for elucidating OTUB1's pro-oncogenic role in the tumor microenvironment.

Current research indicates that the M1 polarization of macrophages is associated with pyroptosis activation [33], whereas the M2 polarization of macrophages is linked to pyroptosis inhibition [34]. This is similar to the results of this experiment. In this experiment, during the polarization of M0 macrophages into M2 in the co-culture group, the expression levels of Cleaved-Caspase-1/4 proteins in HepG2 cells decreased, while the protein expressions of GSDMD, IL-18, and IL-1β increased. This indicates that pyroptosis was inhibited, demonstrating that M2 macrophages suppress pyroptosis in HepG2 cells and thereby promote their proliferation. In the co-culture group with silenced OTUB1, as M0 macrophages polarized toward the M1 type, the expression of Cleaved-Caspase-1/4 protein in HepG2 cells increased, while the protein levels of GSDMD, IL-18, and IL-1β decreased. This indicates enhanced pyroptosis, demonstrating that M1-type macrophages promote pyroptosis in HepG2 cells while inhibiting their growth.

The results of Co-IP and mass spectrometry analysis further suggest that OTUB1 may not function through a single substrate but rather forms an interaction network with multiple candidate proteins involved in cell pyroptosis. Among these, DEAD-box helicase 17 (DDX17) was identified as an inflammasome sensor for retrotransposon RNA [35]; overexpressing Tu translation elongation factor, mitochondrial (TUFM) decreased NLR family pyrin domain containing 3 (NLRP3) activity, thereby inhibiting pyroptosis [36]; Aldehyde dehydrogenase 2 family member (ALDH2) inhibited the NLRP3 inflammasome and pyroptosis by the nuclear factor erythroid 2-related factor 2/reactive oxygen species pathway [37]; YTH N6-methyladenosine RNA binding protein F3/peroxiredoxin 3 (YTHDF3/PRDX3) regulated microglial pyroptosis in neonatal mice [38]. These findings provide a basis for screening and validating key molecules along the “OTUB1-pyroptosis axis” in future studies.

This study still has certain limitations. For example, studies on the liver cancer HepG2 cell line are relatively limited, and the results need to be validated across multiple cell lines; macrophage polarization was primarily assessed based on CD86 and CD206 protein expression, with a lack of additional phenotypic and functional evidence; conclusions regarding pyroptosis were mainly derived from protein expression and electron microscopy morphology at endpoint time points, and the dynamic process requires further investigation; the specific factors regulated by OTUB1 in the pyroptosis pathway require further study; this study is an in vitro cellular experiment, and the role of OTUB1 in the liver cancer microenvironment needs further validation in animal models and clinical samples. Nevertheless, this study still indicates that OTUB1 is an important regulatory molecule linking tumor cell pyroptosis and immune microenvironment remodeling.

Conclusion

Silencing OTUB1 promotes pyroptosis in both HepG2 cells and macrophages and drives macrophages toward an M1-like phenotype, thereby inhibiting the proliferation of HepG2 cells. These findings indicate that OTUB1 may be a key molecule regulating the "pyroptosis–macrophage polarization–liver cancer progression" axis. This study provides a basis for understanding immune regulation in the liver cancer microenvironment from the perspective of the "OTUB1–pyroptosis–macrophage polarization–liver cancer" axis and offers theoretical support for liver cancer immunotherapeutic strategies targeting the OTUB1 or pyroptosis pathways.

Abbreviations

ALDH2: Aldehyde dehydrogenase 2 family member, **BCA**: Bicinchoninic Acid, **CCK-8**: Cell Counting Kit-8, **CD206**: Cluster of Differentiation 206, **Co-IP**: Co-immunoprecipitation, **DDX17**: DEAD-box helicase 17, **DMEM**: Dulbecco's Modified Eagle Medium, **ECL**: Enhanced Chemiluminescence, **GSDMD**: Gasdermin D, **HRP**: Horseradish Peroxidase, **IFN-γ**: Interferon-gamma, **IL-1β**: Interleukin-1β,

LPS: Lipopolysaccharide, **NLRP3**: NLR family pyrin domain containing 3, **OTUB1**: Ovarian tumor deubiquitinase / ubiquitin aldehyde binding 1, **PMA**: Phorbol 12-myristate 13-acetate, **PPI**: Protein-protein interaction, **PRDX3**: Peroxiredoxin 3,

PVDF: Polyvinylidene fluoride, **RIPA**: Radioimmunoprecipitation Assay, **RPMI**: Roswell Park Memorial Institute (medium), **SDS**: Sodium dodecyl sulfate, **siRNA**: Small interfering RNA, **TAMs**: Tumor-associated macrophages, **TUFM**: Tu translation elongation factor, mitochondrial, **YTHDF3**: YTH N6-methyladenosine RNA binding protein 3.

Declarations

Ethics approval and consent to participate: Not applicable.

Consent for publication: Not applicable.

Availability of data and materials: The datasets used and/or analysed during the current study are available from the corresponding author on reasonable request.

Competing interests: The authors declare that they have no competing interests.

Funding: No funding was received.

Authors' contributions: LY conducted the acquisition and analysis of data and was a major contributor to writing the manuscript. HC, XRL, and GXY analyzed and interpreted the findings. CZD and WJ drafted the work and substantially revised the analysis and interpretation of the data. LMN and WXH made substantial contributions to the design of the work and

the interpretation of the data. WXH substantially revised the work. All authors read and approved the final manuscript.

Acknowledgements: Not applicable.

References

1. Bray F, Laversanne M, Sung H, Ferlay J, Siegel RL, Soerjomataram I, et al. Global cancer statistics 2022: GLOBOCAN estimates of incidence and mortality worldwide for 36 cancers in 185 countries. CA Cancer J Clin. 2024 May-Jun;74(3):229–63.
2. Singal AG, Kanwal F, Llovet JM. Global trends in hepatocellular carcinoma epidemiology: implications for screening, prevention, and therapy. Nat Rev Clin Oncol. 2023;20(12):864–84.
3. Seyhan D, Allaire M, Fu Y, Conti F, Wang XW, Gao B, et al. Immune microenvironment in hepatocellular carcinoma: from pathogenesis to immunotherapy. Cell Mol Immunol. 2025;22(10):1132–58.
4. Lu Y, Yang A, Quan C, Pan Y, Zhang H, Li Y, et al. A single-cell atlas of the multicellular ecosystem of primary and metastatic hepatocellular carcinoma. Nat Commun. 2022;13(1):4594.
5. Li D, Zhang T, Guo Y, Bi C, Liu M, Wang G. Biological impact and therapeutic implication of tumor-associated macrophages in hepatocellular carcinoma. Cell Death Dis. 2024;15(7):498.
6. Zhang Y, Han G, Gu J, Chen Z, Wu J. Role of tumor-associated macrophages in hepatocellular carcinoma: impact, mechanism, and therapy. Front Immunol. 2024;15:1429812.
7. Zheng H, Peng X, Yang S, Li X, Huang M, Wei S, et al. Targeting tumor-associated macrophages in hepatocellular carcinoma: biology, strategy, and immunotherapy. Cell Death Discov. 2023;9(1):65.
8. Sun P, Li Z, Yan Z, Wang Z, Zheng P, Wang M, et al. Lenvatinib targets STAT-1 to enhance the M1 polarization of TAMs during hepatocellular carcinoma progression. BMC Cancer. 2024;24(1):922.
9. Wu X, Cao J, Wan X, Du S. Programmed cell death in hepatocellular carcinoma: mechanisms and therapeutic prospects. Cell Death Discov. 2024;10(1):356.
10. Cheng C, Hsu SK, Chen YC, Liu W, Shu ED, Chien CM, et al. Burning down the house: Pyroptosis in the tumor microenvironment of hepatocellular carcinoma. Life Sci. 2024;347:122627.
11. Liu RJ, Yu XD, Yan SS, Guo ZW, Zao XB, Zhang YS. Ferroptosis, pyroptosis and necroptosis in hepatocellular carcinoma immunotherapy: Mechanisms and immunologic landscape (Review). Int J Oncol. 2024;64(6):63.
12. Alishvandi A, Aram C, Shahrivar FF, Kesharwani P, Sahebkar A. Pyroptosis in cancer therapy: a double-edged sword for immune activation and tumor progression. Mol Cancer. 2025;24(1):297.
13. Dai Z, Liu WC, Chen XY, Wang X, Li JL, Zhang X. Gasdermin D-mediated pyroptosis: mechanisms, diseases, and inhibitors. Front Immunol. 2023;14:1178662.
14. Zhu C, Xu S, Jiang R, Yu Y, Bian J, Zou Z. The gasdermin family: emerging therapeutic targets in diseases. Signal Transduct Target Ther. 2024;9(1):87.

15. Li M, Jiang P, Yang Y, Xiong L, Wei S, Wang J, et al. The role of pyroptosis and gasdermin family in tumor progression and immune microenvironment. Exp Hematol Oncol. 2023;12(1):103.
16. Ni L, Chen D, Zhao Y, Ye R, Fang P. Unveiling the flames: macrophage pyroptosis and its crucial role in liver diseases. Front Immunol. 2024;15:1338125.
17. Makuch M, Stepanechko M, Bzowska M. The dance of macrophage death: the interplay between the inevitable and the microenvironment. Front Immunol. 2024;15:1330461.
18. Zhou Z, Song X, Kang R, Tang D. The Emerging Role of Deubiquitinases in Cell Death. Biomolecules. 2022;12(12):1825.
19. Hsu SK, Chou CK, Lin IL, Chang WT, Kuo IY, Chiu CC. Deubiquitinating enzymes: potential regulators of the tumor microenvironment and implications for immune evasion. Cell Commun Signal. 2024;22(1):259.
20. Liao Y, Yang M, Wang K, Wang Y, Zhong B, Jiang N. Deubiquitinating enzyme OTUB1 in immunity and cancer: Good player or bad actor? Cancer Lett. 2022;526:248–58.
21. Wu M, Sun L, Song T. OTUB1-mediated inhibition of ubiquitination: a growing list of effectors, multiplex mechanisms, and versatile functions. Front Mol Biosci. 2024;10:1261273.
22. Wu Y, Mohd Sani SB, Peng K, Lin T, Tan C, Huang X, et al. Research progress of the Otubains subfamily in hepatocellular carcinoma. Biomed Pharmacother. 2024;179:117348.
23. Peng L, Wu T, Liu Y, Zhao D, He W, Yuan Y. OTUB1 accelerates hepatocellular carcinoma by stabilizing RACK1 via its non-canonical ubiquitination. Cell Oncol (Dordr). 2024;47(3):987–1004.
24. Sun C, Cai S, Yang J, Du M, Pan Q, Wang Y, et al. OTUB1 antagonizes TRIM21 to induce deubiquitination of SPHK1 and promote the progression of hepatocellular carcinoma. Oncogene. 2025;44(41):3983998.
25. Yu S, Wang Z, Wang M, Li K, Shang X, Zhao Y, et al. OTU deubiquitinases in cancer pathogenesis and precision therapy. Am J Cancer Res. 2025;15(11):4811–44.
26. Zhu D, Xu R, Huang X, Tang Z, Tian Y, Zhang J, et al. Deubiquitinating enzyme OTUB1 promotes cancer cell immunosuppression via preventing ER-associated degradation of immune checkpoint protein PD-L1. Cell Death Differ. 2021;28(6):1773–89.
27. Deng H, Jia S, Tang J, Rong F, Xu C, Chen X, et al. SET7 methylates the deubiquitinase OTUB1 at Lys 122 to impair its binding to E2 enzyme UBC13 and relieve its suppressive role on ferroptosis. J Biol Chem. 2023;299(4):103054.
28. Sheryazdanova A, Amoedo ND, Dufour S, Impens F, Rossignol R, Sablina A. The deubiquitinase OTUB1 governs lung cancer cell fitness by modulating proteostasis of OXPHOS proteins. Biochim Biophys Acta Mol Basis Dis. 2023;1869(7):166767.
29. Newton K, Strasser A, Kayagaki N, Dixit VM. Cell death. Cell. 2024;187(2):235–56.
30. Wang A, Wang Y, Du C, Yang H, Wang Z, Jin C, et al. Pyroptosis and the tumor immune microenvironment: A new battlefield in ovarian cancer treatment. Biochim Biophys Acta Rev Cancer. 2024;1879(2):189058.

31. Bai L, Xiong J, Chen S, Hu J, Zhang M, Li B, et al. FBXO22 promotes hepatocellular carcinoma progression via paracrine myo-inositol-induced M2-type polarization of macrophages. Int J Mol Med. 2026;57(2):36.
32. Chen JW, Li JY, Feng HQ, Fu LM, Zhou XW, Lin HS, et al. FKBP10 promotes M2 polarization of macrophage via MEK/ERK/CXCL8 axis and facilitates tumor progression in clear cell renal cell carcinoma. Int J Biol Sci. 2026;22(4):1807–33.
33. Xing X, Hu H, Hu H, Chu J, Li S, Han D et al. Quercetin from Penthorum chinense Pursh protects against LPS-induced liver inflammation in chickens via suppressing pyroptosis-macrophage polarization crosstalk. J Ethnopharmacol. 2026;355(Pt A):120665.
34. Pan MM, Ye WH, Zhang RZ, Hu JX, Xie Y, Wang M, et al. Engineering Smart Bimetallic Ionic-Site MOF Nanozyme Nanocomposites for Microenvironment-Responsive Dynamic Therapy of Periapical Periodontitis. ACS Nano. 2026;20(9):7652–69.
35. Minton K. DDX17 identified as inflammasome sensor for retrotransposon RNA. Nat Rev Immunol. 2022;22(2):73.
36. Huang R, Tang X, Liu S, Sun L. Decoding CKD-induced muscle atrophy through the critical role of lncRNA GAS5 and pyroptosis. Mol Ther Nucleic Acids. 2025;36(1):102451.
37. Tong S, Li X, Wang F, Cheng Q, Zhang P, Chen M, et al. ALDH2 Ameliorates Acute Gouty Arthritis Through Inhibiting NLRP3 Inflammasome and Pyroptosis by Nrf2/ROS Pathway. J Inflamm Res. 2025;18:11095–108.
38. Zhang Y, Meng X, Zhao W, Wang G, Zhang C, Tao J, et al. Histone lactylation protects against sevoflurane-induced cognitive impairment by regulating YTHDF3/PRDX3 mediated microglial pyroptosis in neonatal mice. Int Immunopharmacol. 2025;151:114269.

Figures

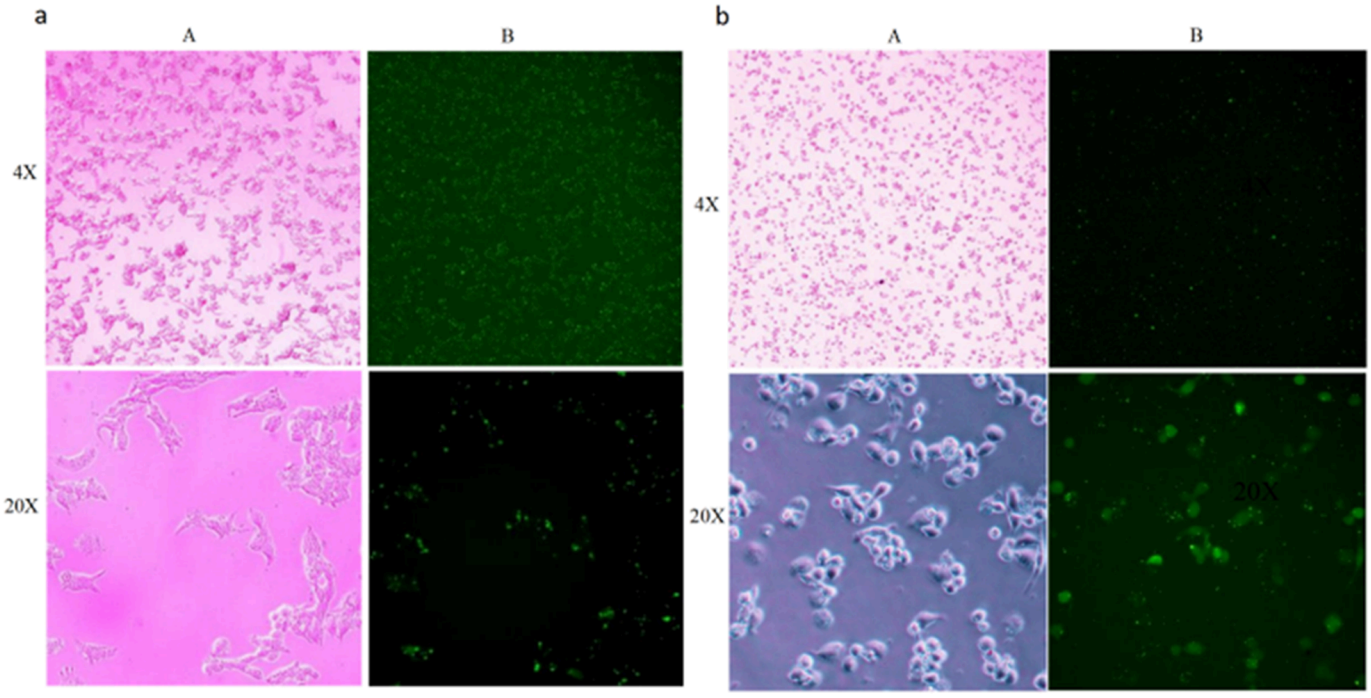


Figure 1

Verification of OTUB1 si-RNA transfection efficiency by immunofluorescence

A: control group, B: transfection group

a. Fluorescently labeled OTUB1 siRNA was transfected into HepG2 cells. b. Fluorescently labeled OTUB1 siRNA was transfected into M0 macrophages. At 10 hours post-transfection, fluorescence microscopy revealed green fluorescent signals in both 4× and 20× fields.

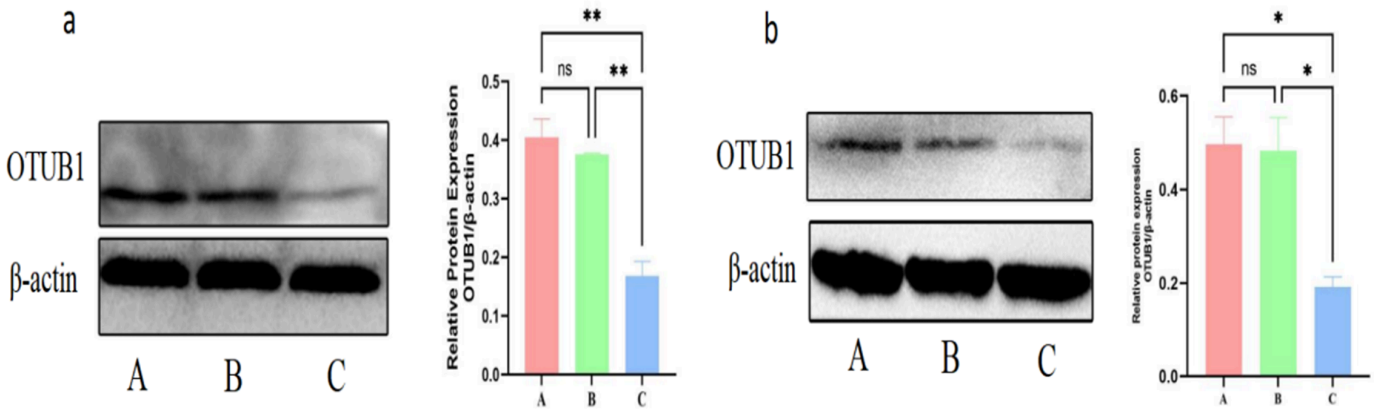


Figure 2

Protein expression of OTUB1 after silencing OTUB1

A: control group, B: negative control group, C: transfection group

a. OTUB1 siRNA and negative control siRNA were transfected into HepG2 cells for 72 hours. b. OTUB1 siRNA and negative control siRNA were transfected into M0 macrophages for 72 hours. OTUB1 protein expression was detected by Western blot. Data are presented as mean ± SEM. Data are representative of at least three independent experiments. *p < 0.05; **p < 0.01.

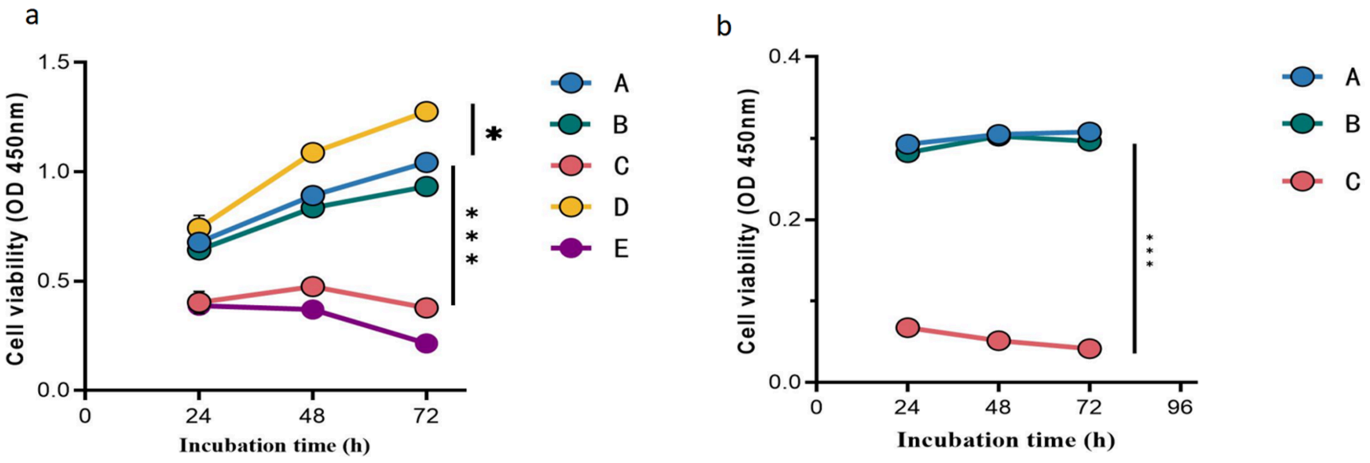


Figure 3

Cell proliferation detected by the CCK-8 assay

A: control group, B: negative control group, C: transfection group, D: co-culture group, E: co-culture transfection group

a. OTUB1 siRNA and negative control siRNA were transfected into HepG2 cells. At 10 hours post-transfection, the medium was changed: groups A, B, and C received complete DMEM; group D received co-culture conditioned medium; group E received co-culture conditioned medium containing OTUB1 siRNA. CCK-8 solution was added at 24, 48, and 72 hours, and after incubation for 2–4 hours, OD450 was measured. The growth curves were plotted. b. OTUB1 siRNA and negative control siRNA were transfected into M0 macrophages. Subsequent treatments (transfection and CCK-8 detection) were the same as those for HepG2 cells. Data are representative of at least three independent experiments. *p < 0.05; ***p < 0.001.

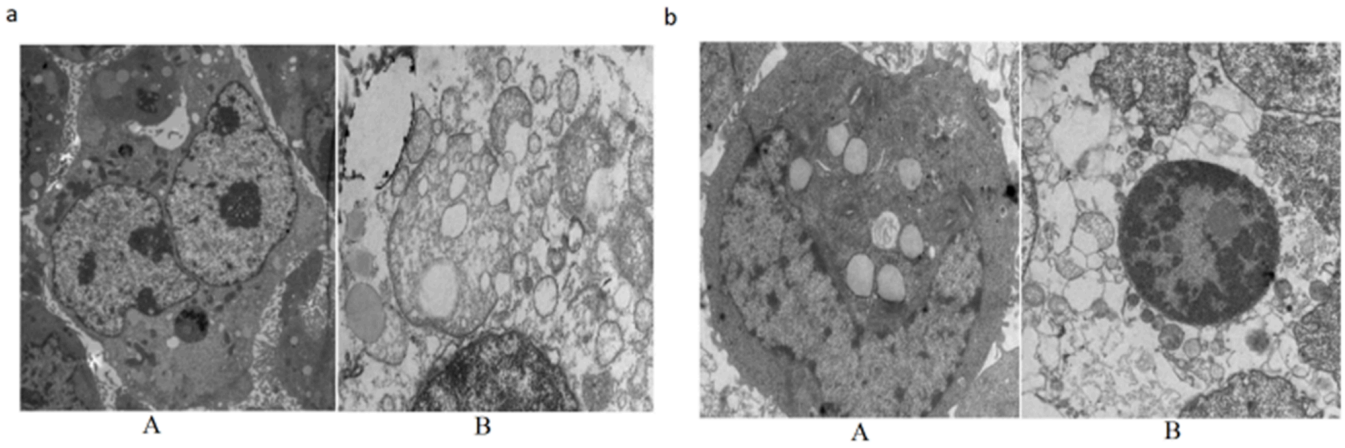


Figure 4

Morphological observation of pyroptosis via electron microscopy

A: control group, B: transfection group

a. OTUB1 siRNA wastransfected into HepG2 cells for 72 hours. b. OTUB1 siRNA wastransfected into M0 macrophages for 72 hours. The cells were collected and observed by transmission electron microscopy.

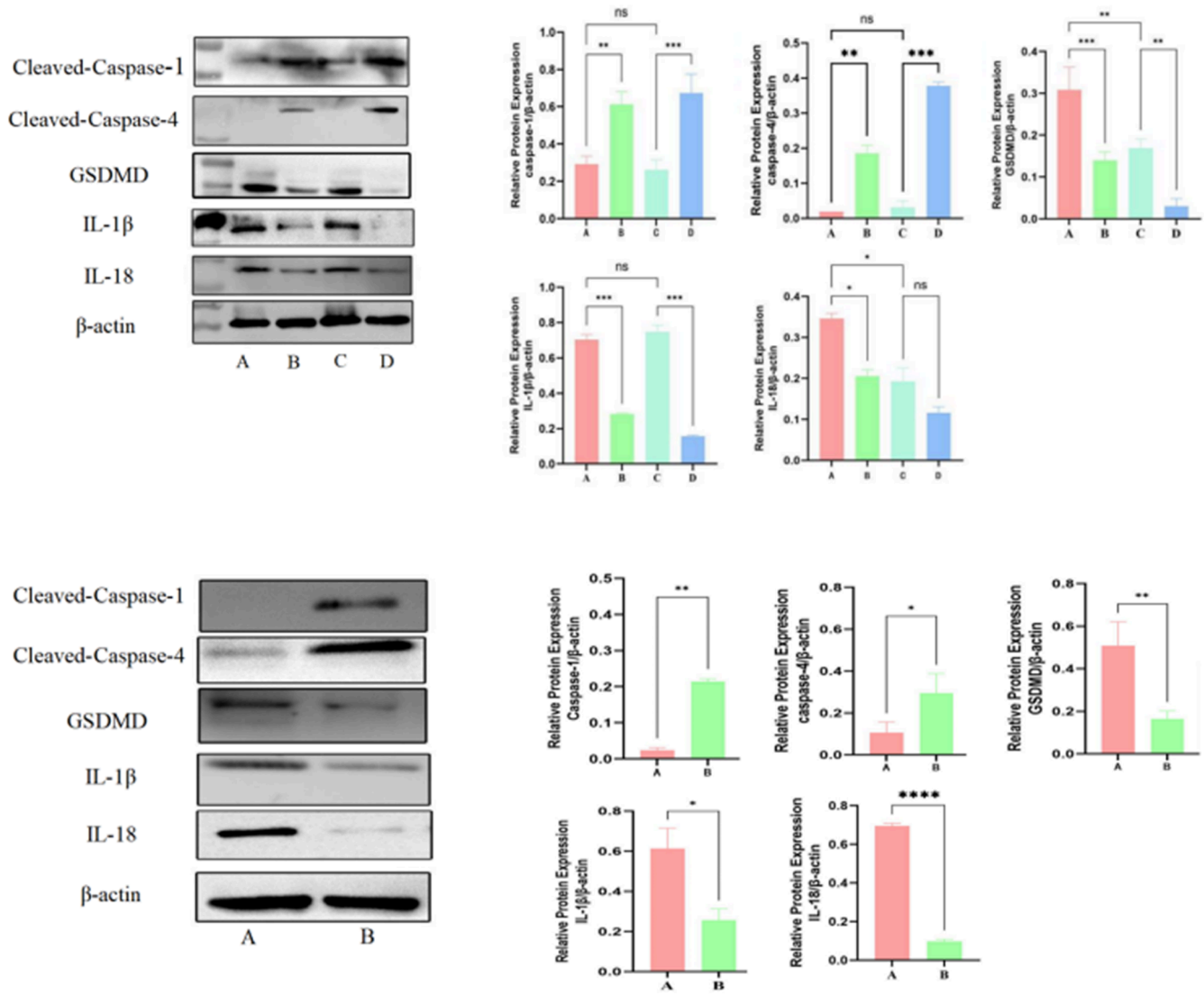


Figure 5

Protein expression of pyroptosis and inflammatory markers after OTUB1 silencing

A: control group, B: transfection group, C: co-culture group, D: co-culture transfection group

a. OTUB1 siRNA wastransfected into HepG2 cells. b. OTUB1 siRNA was transfected into M0 macrophages. At 72 hours post-transfection, proteins were collected from each group, and Western blot was used to detect pyroptosis-related proteins (Cleaved-Caspase-1, Cleaved-Caspase-4, and GSDMD) and inflammatory cytokines (IL-18, and IL-1β). Data are presented as mean ± SEM. Data are representative of at least three independent experiments. *p < 0.05; **p < 0.01; ***p < 0.001; ****p < 0.0001.

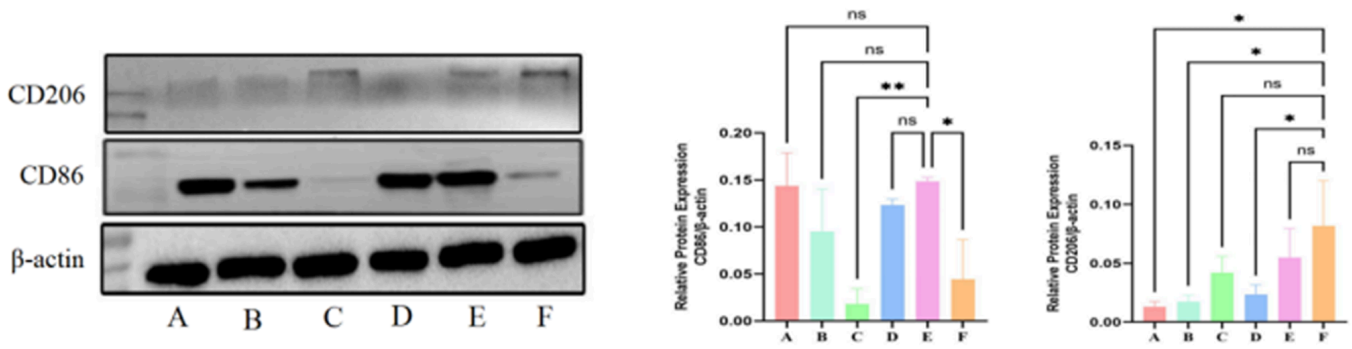


Figure 6

Protein expression of M0 macrophage polarization markers after OTUB1 silencing

A: control group, B: transfection group, C: co-culture group, D: co-culture transfection group, E: M1 macrophage group, F: M2 macrophage group.

OTUB1 siRNA was transfected into M0 macrophages (groups B and D). Adherent M0 macrophages were then incubated with 100 ng/ml lipopolysaccharide (LPS) and 20 ng/ml interferon-gamma (IFN-γ) for 48 hours to induce M1 polarization (E group). Alternatively, adherent M0 macrophages were incubated with 20 ng/ml IL-4 and 20 ng/ml IL-13 for 48 hours to induce M2 polarization (F group). When co-culturing HepG2 cells with M0 macrophages (groups C and D), the two cell types were respectively placed in the upper and lower chambers of a Transwell well, and incubated for 72 hours before use. At 72 hours post-transfection, proteins were collected from each group, and Western blot was used to detect the macrophage markers CD86 (M1 type) and CD206 (M2 type). Data are presented as mean ± SEM. Data are representative of at least three independent experiments. *$p < 0.05$; **$p < 0.01$.

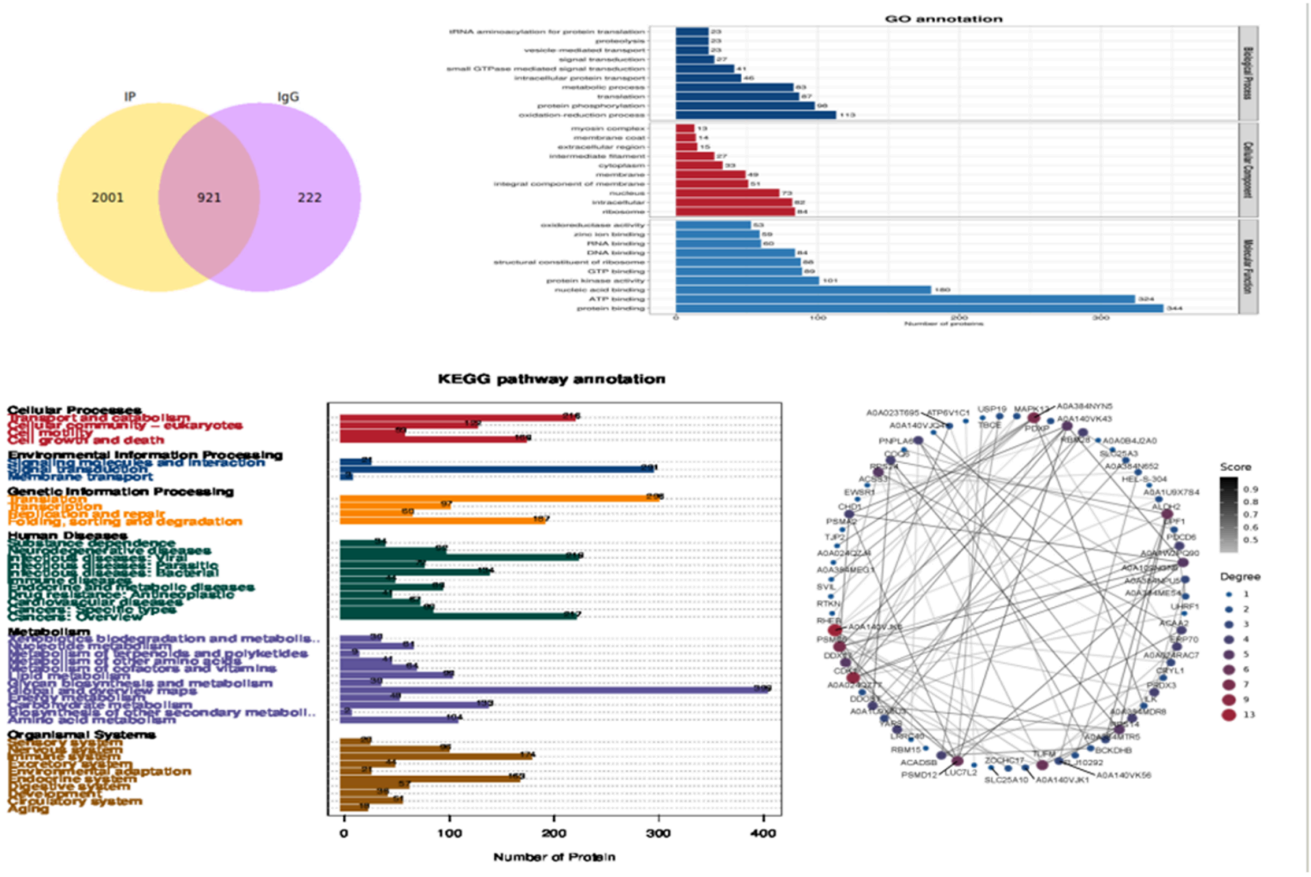


Figure 7

Results of Co-IP and mass spectrometry analysis

The immunoprecipitated products were sent for mass spectrometry analysis. Co-IP results showed that the IP group contained significantly more specific proteins (2922) than the IgG control group (1143), with 921 overlapping proteins. GO annotation analysis indicated that the identified proteins were mainly enriched in biological processes such as redox, transport, and translation, as well as in cellular components including the nucleus, membrane, and cytoplasm. KEGG pathway analysis revealed that the proteins were mainly enriched in cellular processes, genetic information processing, and human disease-related pathways, particularly pathways related to hepatocellular carcinoma development and progression, including cell growth, death, and cancer pathways. Further construction of a protein-protein interaction (PPI) network revealed approximately 59 nodes, with PSMC6, DDX17, LUC7L2, TUFM, RPS14/RPS24, ALDH2, ERP70, ACAA2, PRDX3, and others occupying central positions.